Contribution from Division de Chimie,
D.G.I.-Centre d'Etudes Nucléaires de Saclay, 91190 Gif-sur-Yvette, France

Structural Study and Properties of the Alkali Metal, Nitrosyl, and Ammonium Hepta- and Octafluorouranates(VI)

R. BOUGON,* P. CHARPIN, J. P. DESMOULIN, and J. G. MALM[1]

Received February 3, 1976 AIC60086E

The thermal decomposition of the heptafluorouranates(VI) of the alkali metals is shown to take place in two steps. The first step gives the octafluorouranates(VI) and UF_6, and the decomposition rate is noticeable at temperatures above 100, 130, 150, and 210 °C for the Na, K, Rb, and Cs salts, respectively. The second step for Na_2UF_8 yields pure NaF and UF_6 above 300 °C, whereas the decomposition temperatures for the K, Rb, and Cs salts are above 300, 350, and 400 °C, respectively. Depending on the decomposition conditions, F_2 and M_2UF_7 (M = K, Rb, Cs) or F_2, UF_6, and M_3UF_8 are formed. The heptafluorouranates(VI) of all the cations studied, except for ammonium, were shown to exhibit dimorphism. The parameters of their cubic form were obtained and are as follows: KUF_7; a = 5.22 Å; $RbUF_7$; a = 5.385 Å; $CsUF_7$; a = 5.517 Å; $NOUF_7$; a = 5.334 Å; NH_4UF_7; a = 5.393 Å; $NaUF_7$(fccub), a = 8.511 Å, Z = 4. The x-ray pattern of the low-symmetry form of $CsUF_7$ just below the solid transition temperature (15 ± 1 °C) was indexed with a tetragonal cell where a = 5.50 Å and c = 5.37 Å. The x-ray diagrams of the low symmetry form of the other MUF_7 salts were not indexed, whereas those of the octafluorouranates were indexed with orthorhombic cells. The vibrational spectra of the hepta- and octafluorouranates were found to be very dependent on the temperature, and for the same temperature on the cation size. In the solids at high temperature the disordered F positions are likely to be averaged to give pseudo-D_{5h} and O_h symmetry structures for the UF_7^- and UF_8^{2-} ions, respectively. At lower temperature, as the motions are frozen out, the observed spectra for the hepta- and octafluorouranates arise from structures of symmetry no higher than C_{2v} and D_{2d}, respectively. The ions UF_7^- and UF_8^{2-} were characterized in nitrosyl or cesium fluoride HF solutions, which were found to exchange F^- ions with these anions. Based on observation of the chemical exchange between UF_6 and UF_7^- and on a comparative study of the WF_7^- ion, a fluoride ion transfer mechanism is also found for UF_7^- dissolved in acetonitrile. Some trends observed in this study, like the thermal decomposition temperatures or the relative symmetries, are thought to arise from the differences in the cation–anion interaction. This interaction is stronger with smaller cations, which results in more distorted anions, less ionic U–F bonds, and paradoxically less stable complexes.

Introduction

The syntheses and/or properties of hepta- and octafluorouranates(VI) have been described by several authors.[2-28] In a previous paper, in which the results of a study of the CsF and NOF/UF_6 systems were reported,[27] it was claimed, mainly from vibrational data, that the heptafluoro and octafluoro anions UF_7^- and UF_8^{2-} could have, at least in the solid state, a structure derived from a slight distortion of the idealized bipyramidal (D_{5h}) and cubic (O_h) structures, respectively. In a simultaneous paper,[28] in which x-ray and neutron diffraction work on $NOUF_7$ was reported, it was said that the diffraction patterns could just as well be representative of a monocapped octahedron provided that a statistical occupation of the seventh fluorine atom in the $x'x'x'$ sites was considered. To clear up this apparent discrepancy, a more extensive study was done on this subject in order to obtain a better idea of the structures of the UF_7^- and UF_8^{2-} ions. Some of the corresponding salts were studied both as solids and in solution, using vibrational spectroscopy, x-ray diffraction, and ^{19}F NMR spectroscopy. In addition to the data obtained on the anions themselves or their corresponding alkali metal or nitrosyl salts (such as solid–solid transitions or crystalline structures), some conclusions regarding the effect of the counterion on properties of these salts are given.

Experimental Section

Materials. The compounds UF_6, WF_6, F_2, and HF were purchased from Comurhex; UF_6 was purified from HF by pumping at dry ice temperature; HF was treated with fluorine before use; and F_2 was used without purification. The alkali metal fluorides were purchased from Prolabo and dried either by melting in a crucible followed by cooling in a dry atmosphere or by degassing at 250 °C. NH_4F purchased from Prolabo was used without purification. NOF was produced by first condensing NO, purchased from "l'Air Liquide", and F_2 together at liquid nitrogen temperature in a Monel reactor and then allowing the vessel to warm up to room temperature. In a similar manner, except in Kel-F reactors, the binary mixtures of CsF or NOF with anhydrous HF were obtained by condensing HF onto CsF or NOF. Acetonitrile or SO_2, purchased from Prolabo, was stored over P_2O_5 and introduced onto the sample by vaporization and condensation. Prior to use, propylene carbonate (4-methyl-2-dioxolone, $C_4H_6O_3$), purchased from Koch-Light Laboratories, was stored over 5 Å molecular sieves from Union Carbide International Co., and poured directly onto the sample in the drybox.

Apparatus. The volatile materials were transferred in a vacuum line made for the most part of Monel Metal tubing equipped with valves purchased from F. W. Co. and with differential gauges from "Etudes et Constructions Aéronautiques". For reactors, depending on the experimental requirements, glass bulbs, Kel-F tubes, Monel cylinders, or high-pressure vessels were used, these vessels being attached to the vacuum line through Monel, Kel-F, or Autoclave Engineer high pressure Monel valves. The nonvolatile solid samples were transferred in a drybox containing P_2O_5 as a desiccant.

X-Ray Diffraction Patterns. The Debye–Scherrer powder patterns were taken using a 114-mm diameter Philips instrument with copper Kα radiation (1.5418 Å). The samples were contained in quartz capillaries (~0.5 mm) and studies in the temperature range +40 to −180 °C were made possible by use of a Meric cryostat.

Spectra. Infrared spectra were recorded with a Beckman Model IR 9 and a Perkin-Elmer Model 457 in the ranges 4000–400 and 4000–250 cm^{-1}, respectively.

A few measurements were also made in the far-infrared region (400–40 cm^{-1}) using an FS 720 spectrophotometer. Powders were pressed between two thin plates of AgCl 12 mm in diameter or as a Nujol mull between plates of KBr or polyethylene disks. Solutions were studied using Barnes polyethylene molded cells (path length 0.2 mm). These cells were filled in the drybox with a Teflon syringe. The Raman spectra were recorded with a Coderg Model T 800 using the 514.5 nm line of a Model 165 Spectra Physics laser as the exciting light. For these spectra, the neat powders were contained in glass capillaries (~2 mm) whereas the solutions were contained in KelF or FEP Teflon tubing (6 mm i.d.). The low-temperature spectra were obtained either with an Air Liquide cryostat for the liquid helium temperature range or a Coderg cryostat for temperatures above liquid nitrogen, in which cases the solid samples were contained in 30 cm long, 4 mm o.d., glass tubes or 8 mm long, ~2 mm o.d. capillaries, respectively. The frequency accuracy was estimated to be approximately ±3 cm^{-1} for the infrared spectra and ±1 cm^{-1} for the Raman spectra. The visible and near infrared spectra which were used for a further identification of the residues from the thermal decomposition of the octafluorouranates were recorded on a Cary 14 instrument. The corresponding powders were studied as Nujol mulls between two CaF_2 plates.

The ^{19}F NMR spectra were obtained on a Varian NV 14 spectrometer operating at 56.4 MHz equipped with a variable temperature probe and an extended scale allowing observation to be made as far as −675 ppm downfield from the $CFCl_3$ resonance. Furthermore, a Schlumberger frequency generator was used to shift the frequency scale even further so that the scale was extended to −953 ppm. The resonance frequencies were determined with a Schlumberger frequency counter. $CFCl_3$ was used as an external reference and the spectrometer was locked on this resonance. For these spectra the solutions were contained in a 6 mm o.d. Kel-F tube hot-pinched and placed into a 8 mm o.d. calibrated NMR tube containing a small amount of $CFCl_3$. The chemical shift accuracy was estimated to be ±0.1 ppm.

Preparations. The complexes $NOUF_7$ and $(NO)_2UF_8$ were prepared according to the methods previously described.[27] That is, UF_6 was reacted with a large excess of liquid NOF to get $(NO)_2UF_8$; $NOUF_7$ was obtained by reaction between stoichiometric amounts of NOF and UF_6 at dry ice temperature. The alkali metal fluoride–UF_6 complexes were also prepared as previously described[27] for $CsUF_7$ and Cs_2UF_8. That is, an excess of liquid UF_6 was reacted with the alkali metal fluorides to prepare the heptafluorouranates; controlled thermal decomposition of the MUF_7 salts (M = Na, K, Rb, Cs) under pumping yielded the octafluorouranates. To obtain the pure heptafluorouranates, however, it was found necessary to grind the mixture several times during the synthesis; after the MF–UF_6 mixture has been left at the chosen temperature for several hours, the excess UF_6 was pumped off at room temperature and the solid residue was ground in the dry box and then reacted further with UF_6. This procedure was repeated until pure MUF_7, as checked by its Raman spectrum, was obtained.

As already reported[19,21,27] the formation of the octafluorouranates is favored at high temperature, so for all the syntheses, the temperature was kept in the range 65–100 °C. It was found that under pumping the temperature at which decomposition of the heptafluorouranates was noticeable was 100, 130, 150, and 210 °C for the Na, K, Rb, and Cs salts, respectively. The NH_4UF_7 complex[10] was prepared by reaction between an excess of gaseous UF_6 and NH_4F at room temperature, whereas $(NH_4)_2UF_8$ was obtained by using only the stoichiometric amount of UF_6. For some of the experiments performed with an excess of UF_6, a fast decomposition with the production of NH_4UF_6 spontaneously took place and consequently the decompositions of the ammonium salts were not studied. The decompositions of the alkali metal salts were studied either with an MCB Arion microcalorimeter connected to a homemade microsublimation–microdesorption apparatus, or a Monel reactor connected to the vacuum line.

The purity or identification of the compounds were checked or made by x-ray diffraction and vibrational spectroscopy and comparison was made with literature data when available. The identification of the new complexes was further confirmed by chemical analyses.

Results and Discussion

Synthesis and Thermal Stability. The complexes MUF_7 and M_2UF_8 (M = Na, K, Rb, Cs, NO, NH_4) were prepared as pure solids. Some attempts were made to extend this series to the Li salt without success. A new form of $NaUF_7$ (cubic) was isolated in an attempt to grow single crystals in liquid UF_6 at 200 °C. Unfortunately this new form was unable to be reproduced either at temperatures between 65 and 220 °C or by quenching at −196 °C. From an analogy with the data on the phase changes obtained with the other complexes, this cubic form is thought to be metastable at room temperature, whereas at higher temperature where it could be stable, the decomposition rate of $NaUF_7$ into Na_2UF_8 prevents its reproducible isolation. As for the "normal" form, the decomposition of cubic $NaUF_7$ is rapid at 100 °C liberating UF_6 and producing Na_2UF_8. The latter is decomposed at 300 °C to give UF_6 and pure NaF, with no trace of any reduced form of uranium.

Conversely, the thermal decompositions of the other M_2UF_8 complexes (M = K, Rb, Cs, NH_4) take place leaving a reduced form of uranium. As already pointed out, the ammonium salts are sometimes spontaneously reduced during their preparations and their thermal stabilities were not further studied. The stabilities of the other complexes were found to increase with the atomic weight of the cation. K_2UF_8 decomposes above 300 °C, Rb_2UF_8 above 350 °C, and Cs_2UF_8 only above 400 °C. Under the conditions of decomposition for these compounds (≤450 °C) the uranium was normally found in the pentavalent state. Only in some cases at the highest of temperatures was the uranium found in the tetravalent state. The thermal decomposition products UF_6, F_2, M_2UF_7, and M_3UF_8 were produced in varying ratios depending on the temperature, pumping rate, and amount of starting material.

The study of the decomposition mechanism was restricted to the cesium salt. In this case Cs_2UF_7 is first produced, according to

$$Cs_2UF_8 \rightarrow Cs_2UF_7 + {}^1/_2F_2 \quad (1)$$

whereas the formation of Cs_3UF_8 and UF_6 is explained through

$$3Cs_2UF_7 \rightarrow 2Cs_3UF_8 + [UF_5] \quad (2)$$

$$^1/_2F_2 + [UF_5] \rightarrow UF_6 \quad (3)$$

(In these equations $[UF_5]$ stands for UF_5 itself or its thermal decomposition residue and of course (3) has to be corrected according to the decomposition stage.)

At completion, the procedure may be written as

$$3Cs_2UF_8 = 2Cs_3UF_8 + F_2 + UF_6 \quad (4)$$

The mechanism proposed above is suggested because of the following observations: (i) With a small amount of initial solid, like that used in the microcalorimeter (~50 mg) or in the Raman capillaries, Cs_2UF_8 was transformed into Cs_2UF_7 by heating the sample up to 450 °C in the microcalorimeter or by heating it with the high-density energy of the laser beam. In the microcalorimetry experiment F_2 was the only gas detected. (ii) With a larger amount of solid, on the order of a few grams, both UF_6 and F_2 were given off when the sample was heated to 450 °C in a nickel vessel in vacuo. Fluorine was the first gas given off and the solid residue was found to be Cs_3UF_8. The apparent discrepancy between the two results is thought to be due to the difference in the escape rate of F_2. With a larger amount of initial solid, this rate is slowed down by diffusion through the solid in such a way that F_2 is able to react with UF_5 to produce UF_6. As a result, reaction 2 can then go to completion with the formation of Cs_3UF_8 as the solid residue. This latter reaction has been proved by heating Cs_2UF_7 for 65 h in vacuo at 450 °C in a Monel reactor, which results in the formation of a few percent of Cs_3UF_8 and an ill-defined phase localized near the surface of the solid. From its x-ray powder pattern, this phase is attributed to UF_x ($4 < x < 5$). These findings are consistent with the preceding observations, and the presence of fluorine in the solid is certainly necessary to drive reaction 2 to completion through the fluorination of $[UF_5]$.

MF (M = NO, Cs), HF, UF_6 Systems. These systems were studied in the hope of obtaining information on UF_7^- and UF_8^{2-} as pure species without the disturbing effects such as those taking place in the solid state. As previously mentioned[27] $NOUF_7$ is decomposed in pure HF but is soluble in the NOF·3HF mixture. With the addition of HF to this solution, UF_6 is displaced from $NOUF_7$.

These observations are consistent with the following equilibria

$$UF_7^- + HF \rightleftarrows UF_6 + HF_2^- \quad (5)$$

$$NO^+ + HF_2^- \rightleftarrows NOF + HF \quad (6)$$

These equations were also found to hold when NO was replaced by Cs. Moreover, if the concentration of MF (M = NO, Cs) is increased, the equilibria are shifted such that the number of ligands around the uranium atom is increased and

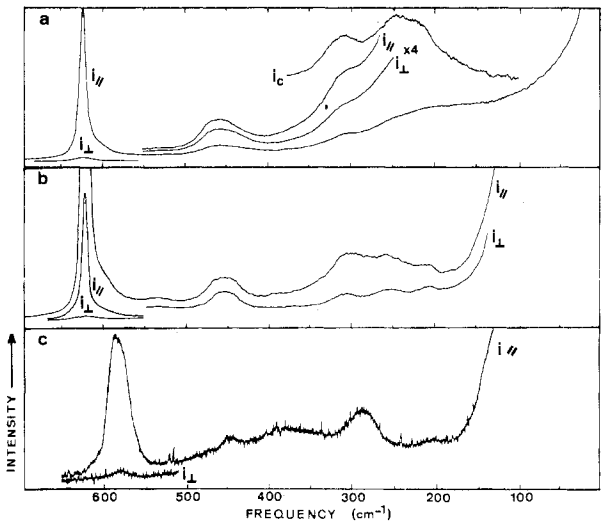

Figure 1. Raman spectra of UF_7^- and UF_8^{2-} ions: (a) $NOUF_7$ in NOF·3HF solution (spectral slit width 2.4 cm^{-1}); (b) $CsUF_7$ in CsF/HF solution (spectral slit width 2.4 cm^{-1}); (c) Cs_2UF_8 in CsF/HF solution (spectral slit width 4.8 cm^{-1}). i_c refers to the calculated intensity (the solvent contribution is removed). $i_{\parallel}$ and $i_{\perp}$ refer to the polarization directions. In (c) the band at 450 cm^{-1} is mainly due to Kel-F.

the UF_8^{2-} ion is formed. The identification of this latter ion in solution was made by comparison of its Raman spectrum to one obtained for the solid. The corresponding equilibrium can then be written as

$$UF_7^- + HF_2^- \rightleftarrows UF_8^{2-} + HF \quad (7)$$

Typical Raman spectra of solutions containing the UF_7^- or UF_8^{2-} ions are shown in Figure 1. The corresponding frequencies are listed in Tables I and II, together with those of the solids. The bands are broad probably as a result of solute–solvent interactions and interatomic lengths and angle distributions (see discussion on solid state data). On the other hand, apart from the effect of the MF concentration on the equilibria written above, this MF concentration has an effect on both the number and the location of the bands of each species. It is convenient, for instance, to consider each species' highest stretching frequency which, in addition to being polarized, is also the most intense and best defined. For pure UF_6 in HF this band is found at 666 cm^{-1} (the half-line width of which is 5 cm^{-1} ($\Delta\bar{\nu}_{1/2}$)). Upon the addition of CsF in the molar ratio[29] of CsF:UF_6:HF corresponding to 8.7:0.226:100, a new band appears at 630 cm^{-1}, $\Delta\bar{\nu}_{1/2}$ = 25 cm^{-1}, which is assigned to UF_7^- by comparison with a spectrum of the solid. With a further increase in the amount of CsF (e.g., CsF:UF_6:HF as 28.6:0.157:100) this band is shifted to 621 cm^{-1} ($\Delta\bar{\nu}_{1/2}$ = 10 cm^{-1}) while a shoulder appears at 600 cm^{-1}. At higher CsF concentration the 621 cm^{-1} band progressively disappears, while the shoulder is changed into a band located at 587 cm^{-1} ($\Delta\bar{\nu}_{1/2}$ = 30 cm^{-1}). This last band is assigned to the UF_8^{2-} species. In the solid samples of UF_6, MUF_7, and M_3UF_8, such a decrease in frequency is explained[27] by an increase of the electronic charge on the coordination sphere of the uranium atom. It is then quite reasonable to assume that such an increase in electronic charge also occurs in solution from solute–solvent interactions. The HF_2^- ion, the concentration of which increases with the amount of CsF, is most likely responsible for this interaction.

The equilibria 5 and 7 written above were not studied from a quantitative point of view, but their existence is consistent with the ^{19}F NMR study performed on these solutions. The data reported in Table III concern the CsF/UF_6/HF solutions. It is seen that when UF_6 is absent, an increase in the CsF concentration shifts the resonance downfield, whereas with an increase in the CsF/UF_6 molar ratio, this line is shifted upfield. In any case, the exchange rate was too rapid to give separate signals, thus no structural information was available from this NMR study.

Concerning this structural aspect, it may be recalled that the UF_7^- ion in solution exhibits rather broad Raman bands. For the solid samples, however, the presence of five bands can be estimated from the spectra so that a pentagonal bipyramidal model may be valid for the fluorine arrangement about uranium. In the Raman spectra of solutions at higher MF concentrations, a further increase in the solute HF_2^- interaction would make an anion distortion more important and would account for the appearance of the weak 535-cm^{-1} Raman line, the infrared counterpart of which is strong for the solid. As far as the octafluoroanions are concerned, their spectra in solution were too poorly resolved to give any structural information. Furthermore, no infrared spectra were obtained on either the heptafluoro or octafluoro anions in solution due to experimental difficulties inherent with their corrosive natures.

Organic Solutions. Acetonitrile and propylene carbonate (PC) were found to be the most suitable organic solvents capable of dissolving the compounds studied here. In acetonitrile for instance, the KUF_7 complex was soluble and the solute/solvent molar ratio reached ~5%. The complexes $CsUF_7$ and $RbUF_7$ were less soluble and the octafluorouranates were too sparingly soluble to allow NMR or vibrational studies to be done. The vibrational data obtained from a KUF_7/acetonitrile solution are listed in Table I. From the number of bands observed together with their appearance in both the Raman and infrared spectra, it is clear that a D_{5h} structural model is not appropriate and the spectra are closer to those observed for solid KUF_7. Regarding the results from the MF/HF/UF_6 system, a possible disturbing effect of the solvent on the actual structure of the free anion must be borne in mind. This idea is supported by the lowering of the highest U–F stretching frequency of the solute in acetonitrile when compared to the corresponding frequency found in the solid; in addition, the NMR data indicate that UF_7^- is exchanging F^- ions with UF_6 in CH_3CN. As mentioned below, the NMR observations are explained through extra coordination of the uranium atom by acetonitrile, giving rise to a possible disturbing effect on the surroundings of the fluorine atoms. The ^{19}F NMR spectra of solutions of KUF_7 dissolved either in PC or in acetonitrile have been recorded. In each case only one band was observed, the location of which was found to be constant in the +10 to −45 °C temperature range. In acetonitrile for a 4.5% solute/solvent molecular ratio, the chemical shift from $CFCl_3$ and the half-line width was −605.7 ppm (400 Hz) and −605.9 ppm (600 Hz) at +10 and −45 °C, respectively. These chemical shifts are consistent with the mean values observed[27] for $CsUF_7$ and $NOUF_7$ as solids, i.e., −575 and −634 ppm, respectively. The line is likely due to an exchange between the different types of fluorine atoms in UF_7^-, and some further experiments were made in order to understand the mechanism of this exchange. First of all, consistent with either an inter- or intramolecular exchange, the line width was found to be significantly increased with a decrease in temperature. Moreover UF_6, which gives a signal around −745 ppm in acetonitrile,[30] gives only one signal in the presence of UF_7^- instead of two, whereas in the Raman experiment, signals for both UF_6 and UF_7^- are observed. The NMR signal is located at −701 ppm at +10 °C for KUF_7/UF_6 at a molar ratio equal to 23.5%. At lower temperatures UF_6 precipitates out and the signal is shifted upfield (−672.1 ppm at −10 °C). The two species UF_6 and UF_7^- are definitely exchanging F^- ions in acetonitrile. It is worth noting that such

Table I. Vibrational Data[a] for $NOUF_7$ and $CsUF_7$ in CsF/HF or NOF/HF Solution, for KUF_7 in Acetonitrile Solution, and for $NaUF_7$, KUF_7, NH_4UF_7, and $RbUF_7$ in the Solid State

$NOUF_7$, Raman		$CsUF_7$, Raman		KUF_7														
	NOF, 3HF		CsF,	Acetonitrile[c] soln		Solid[d] Raman					$NaUF_7$, solid, Raman			NH_4UF_7, solid,	$RbUF_7$, Solid Raman		
Solid[b]	solution	Solid[b]	nHF soln	Raman	Ir	I	II	III	IV	Ir	Cub. phase	Low sym	−180 °C	Raman	RT	−170 °C	Ir
627	626 p	622	621 p	620 (10) p	617 vw	626	625	623	625	626 w	633 (10)	635 (10)	636	625 (10)	625 (10)	624 (10)	625 w
			600 sh[e]						602							593 (0.1)	
							580		594	580 sh	554 (<0.1)	554 (0.1)	554			546 (<0.1)	550 s, br
			535[e]	540 (0.1)	535 vs		541	544	545	540 s, br	542 (0.1)	541 (0.2)	540				
				523				517	520			515 (<0.1)	516		520 (<0.1)	517 (<0.1)	
							496	502	500	497 s, br						503 (0.1)	482 w
									463			461 (0.8)	463			457 (0.6)	457 m
	460 dp	462 sh	455 dp	454 (0.8) dp	456 sh		456	455	457	457 w	450 (0.9)						
446 sh		444				440	438	440	441			442 (0.7)	441	447 (1.25)	443 (0.9)	442 (1)	442 w
434									438	438 w		429 (0.3)	430				
310	308 p	312		312 (0.3)	310	312	315	311	313	314 w	310 (0.8)	310 (1.1)	312	314 (0.55)	310 (0.5)	311 (0.7)	
			305 p	294 sh	300		300			296 sh			305 sh			304 sh	
									267								
					264		253	253	255	256 w						254 (0.5)	
240	245	249	250 dp	247 (0.3)	246	247			248		242 (1.1)	242 (1.5)	243	250 (0.76)	248 (0.5)	242 sh	
							231	232	232	234 s, br						230 (0.3)	230 m
					222			212	215		216 sh	215 (0.6)	218	215 (1.74)	215 (0.4)	207 sh	210 m
210	215	211	210 dp	210 (0.2)		209	206	201	198	202 s, br	203 (1.2)	204 sh		195 (1.53)		201 (0.4)	
									150	140 m							
									131				111				
							80 (L)	100	96 (L)	100 (L)		104	91 (L)			100	
								31 (L)	32			54 (L)	57			53 (L)	
												34	35			35	

[a] Frequencies are given in cm^{-1}. All Raman intensities are uncorrected. Only internal or lattice (L) vibrations are listed. Unless specified, spectra were recorded at room temperature. [b] From ref 27. [c] Acetonitrile has an ir and Raman active band at 380 cm^{-1} which is not listed here. [d] Evolution of the Raman spectrum with temperature: I, above room temperature; II, at room temperature after aging or thermal activation; III, at room temperature without thermal activation; IV, At ca. −140°. [e] Only observed for high F^- concentration (see text).

Table II. Vibrational Data[a] for the Sodium, Potassium, Nitrosyl, Ammonium, Rubidium, and Cesium Octafluorouranates

Na_2UF_8, Raman	K_2UF_8		$(NO)_2UF_8$				$(NH_4)_2UF_8$, Raman	Rb_2UF_8, Raman	Cs_2UF_8			
	Raman		Raman			NOF/HF soln[b] (Raman)			Raman			CsF/HF soln (Raman)
	>RT	Ir	−250 °C	Ir					−200 °C	Ir		
607 (10)	591 (10)	598 (10)	598 m	590 (10)	591 (10)	590 sh	595 p	592 (10)	590 (10)	583 (10)	584 (10)	586 w	587 p
						534 sh						578 w	
						510 s						508 s	
		506 sh	510 s, br			498 sh							
		494 (0.3)											
		483 (0.3)						477 (0.1)		474	477 (0.3)	464 sh	470
	470 (0.2)	463 (0.3)	460 sh	460 (0.1)	473 (0.1)		470 (0.3)	454 (0.1)		450	452 (0.3)		
440 (0.2)		441 (0.2)			448 (0.2)		420 (0.3)	425 (0.1)			418 (0.2)		
410 (0.6)	405 (0.5)	408 (0.5)		407 (0.3)	409 (0.4)			400 (0.4)		395 (0.4)	398 (0.4)		390
372 (0.5)		392 sh	390 sh					387 (~0.1)			382 (0.2)		
343 (0.7)	326 (1.5) (L)	325 (1.5) (L)		328 (0.9) (L)	330 (1) (L)		321 (1.4) (L)	323 (1.2) (L)		321 (1.1) (L)	323 (1) (L)		
303 (1.1)	292 (1.4)	295 (1)	294 vw										
284 (1.1)		286 sh		285 (1)	284 (1.4)		286 (1.5)	288 (1.0)		282 (1.1)	282 (1.3)		285
			260 s					282 (1.0)				270 m	
			232 s, br			208 w						176 m	
170 (0.7)	120 (L)	126		100		160 m	112	118		108	112 (L)		
141 (0.3)		43 (L)		41 (L)			38 (L)	38 (L)		36 (L)			

[a] Frequencies are given in cm^{-1}. All Raman intensities are uncorrected. Only internal or lattice (L) vibrations are listed. Unless specified, spectra were recorded at room temperature. [b] Due to the bands of the solvent, the bands of the solute were not observable below ~500 cm^{-1}.

Table III. ^{19}F NMR Data[a] on the $CsF/UF_6/HF$ Solutions

Molar ratio[b]				$\delta(CFCl_3$, ext.),[c] ppm	Line width, Hz
CsF	UF_6	HF	CsF/UF_6		
8.7	0	100		185.6	52
8.7	0.226	100	39.5	166.2	124
28.6	0	100		167.0	68
28.6	0.157	100	18.2	150.9	840
28.6	0.212	100	13.5	144.2	1 050

[a] Temperature +10 °C. [b] See ref 29. [c] Chemical shift values as positive upfield from the $CFCl_3$ resonance.

a comparable fluoride transfer has been recently reported by Prescott et al.[31] for mixtures of WF_6 and TlF or CuF_2 in CH_3CN solution. In addition it has been found here that KWF_7, prepared by reaction between KF and WF_6 in SO_2 and identified in solution by comparison with its Raman spectrum in the solid state, was slightly soluble in both acetonitrile and PC (~2 % M) and gave a narrow resonance at −142.4 ppm (1.2 Hz) and −143.4 ppm (1.7 Hz) at +10 °C in CH_3CN and PC, respectively. The interesting point was the lack of ^{19}F–^{183}W satellite peaks. From this point and the assumption that the coupling is not less than a few hertz (44 Hz for neat WF_6) it was concluded that the bonds in WF_7^- are periodically broken and re-formed through some intermolecular process in CH_3CN and PC. Surprisingly, the exchange still takes place in the supercooled phase of PC where at −70 °C, for instance, the signal remains unique at δ −143.4 ppm (5.6 Hz). This demonstrated intermolecular exchange for the WF_7^- ion may also be reasonably assumed to take place for the similar UF_7^- ion. A possible way to explain this exchange is to assume that the solvent is a strong enough donor to replace a fluoride ion in the anion. This assumption is consistent with the solvation found for UF_6 in CH_3CN[30] and with the above reported exchange between UF_6 and UF_7^- and again with the syntheses reported by Prescott et al.[31,32] Best understood in the case of acetonitrile, the equilibria responsible for the exchange could be schematically written as

$$CH_3CN: + UF_7^- \rightleftarrows [CH_3CN: UF_7^-] \rightleftarrows [CH_3CN: UF_6] + F^- \quad (8)$$

The solvation of both K^+ and F^- is not taken into account; but these equilibria are most certainly shifted toward the left, since no band that could be attributed to UF_6 is seen in the Raman spectrum of this solution.

Solid State Study. As pointed out by Muetterties,[33] the structural determinations of the molecular geometries ought to take into account a possible nonrigid structure. Muetterties mentioned that inorganic chemistry is rich in such molecules where such dynamics take place. It is worthy to note that seven and eight coordinate species are found in this connection. One of the main observations which have been made during this study was the thermal effect on the observed vibrational spectra of the hepta- and octafluorouranates. Furthermore, that a "molecular" motion is taking place in these salts has been previously demonstrated by ^{19}F broad line NMR spectroscopy.[34–36] Both the UF_7^- and UF_8^{2-} groups have been found to reorient and the ease with which they reorient increases with the increasing size of the associated cation. The reorientation motion model is not accurately known but it certainly allows an internal exchange of the fluorine atoms for which a fast exchange and relatively long time scale of observation do not allow structural determinations. This is specially true for the NMR technique for which[34–36] the difference in the shielding of the fluorine atoms of UF_7^- vanishes at high temperature. On the other hand, with shorter observation time scales an instantaneous view of the motion effect is represented by disorder. Sometimes for x-ray diffraction data for instance, the resultant disorder of position or orientation of some of the atoms has to be assumed to be

averaged to account for the symmetry of the crystal field to be compatible with the symmetry of the motif. These atoms are then said to have a "statistical occupation", i.e., a partial occupation rate. In the same way this motion effect results in a larger distribution of the bond lengths and angles around the equilibrium position, giving in turn ill-defined vibrational levels. From this, both the Raman and infrared bands are then expected to be broad. The experimental data obtained on the solids are all consistent with such motion effects.

X-Ray Diffraction Study. Some of the structural data for the heptafluorouranates have been given previously; $CsUF_7$ has been found to exist under two forms by Sadikova et al.,[24] i.e., a cubic form at room temperature and a tetragonal form at 250 °C. On the other hand, Geichman et al.[14] have found a pseudocubic symmetry cell for $NOUF_7$ at room temperature. The diagram of $NaUF_7$ has not been indexed[18] whereas a cubic phase has been found for KUF_7,[26] $RbUF_7$,[26] and NH_4UF_7.[10] All the compounds studied here except for NH_4UF_7 can have two crystalline forms: a cubic and a low-symmetry form, the latter also being the lower temperature form.

The parameters of the cubic forms were found to be as follows: KUF_7, $a = 5.22 \pm 0.01$ Å; $RbUF_7$, $a = 5.385 \pm 0.005$ Å; $CsUF_7$, $a = 5.517 \pm 0.005$ Å; $NOUF_7$, $a = 5.334 \pm 0.007$ Å; NH_4UF_7, $a = 5.393 \pm 0.005$ Å; and $NaUF_7$ (fccub) ($Z = 4$), $a = 8.511 \pm 0.008$ Å. Neither the transition temperature nor the x-ray powder diagrams of the low-symmetry forms have been clearly determined, except for the cases of $NOUF_7$[28] (transition temperature) and $CsUF_7$ (transition temperature and x-ray powder diagram). The solid transition of $CsUF_7$ occurs at 15 ± 1 °C and its low-symmetry form x-ray diagram is indexed with a tetragonal cell, with $a = 5.30$ Å and $c = 5.37$ Å. From the noticeable shrinkage of one of the cubic axes, the decrease in volume of the unit cell reaches ca. 2.4% at the transition point.

The x-ray data of the octafluorouranates, except in the case of Na_2UF_8,[18] were previously unknown. The powder diagrams of the other salts were indexed with an orthorhombic cell. The corresponding x-ray data and parameters are given in Table IV. These indices were determined through comparison with isostructural complexes like Rb_2UF_7,[37] K_2TaF_7,[38] and K_2NbF_7[38,39] and also from the structural parentage[40] between the complexes $(NO)_2ReF_8$ and $(NO)_2WF_8$ prepared by Beaton[41] as well as from the complexes M_2ReF_8 (M = Rb, K) described by Ippolitov and Koz'min.[42] Since structures of both the K_2NbF_7 and M_2ReF_8 complexes have been thoroughly described, the isomorphism allowed a clear-cut indexing of the octafluorouranate patterns. It is worth adding that the data reported by Malm et al.[18] on Na_2UF_8, which were based on a single crystal study, have shown that this compound has a body-centered tetragonal phase; consequently it does not belong to the same structural type as the other octafluorouranates.

Vibrational Spectroscopy. Vibrational data obtained for the MUF_7 and M_2UF_8 complexes (M = Na, K, Rb, Cs, NO, NH_4) are listed in Tables I and II, respectively. The Raman spectra were found to be much more informative than the infrared spectra because the latter for the most part were broad and ill-defined. Therefore, the infrared frequencies for only some of the complexes are listed in these tables and the spectra are not shown. The temperature effect on the Raman spectra was particulary spectacular for KUF_7 and is displayed in Figure 2 and Table IV. For those temperatures estimated to be higher than 40 °C (cubic phase range), the Raman spectrum is closely related to those obtained for the UF_7^- ion in solution and only five bands are apparent (see Figure 2, spectrum I). This type of spectrum with only minor changes has been found for all the heptafluorouranates in their cubic

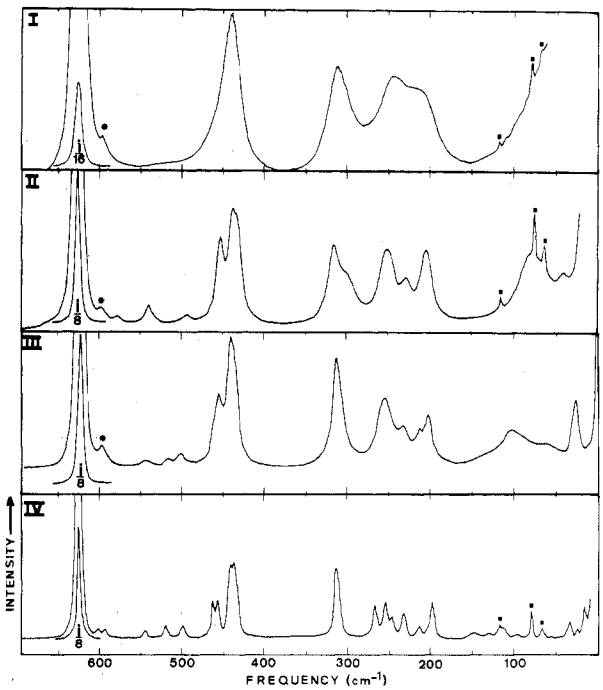

Figure 2. Raman spectra of solid KUF_7: (I) above room temperature (ca. +40 °C) (spectral slit width 3.2 cm^{-1}); (II) at room temperature after aging or thermal activation (spectral slit width 3.2 cm^{-1}); (III) at room temperature (spectral slit width 2.4 cm^{-1}); (IV) at ca. −140 °C (spectral slit width 2.4 cm^{-1}). The band with an asterisk is due to a small amount of K_2UF_8 and the bands with solid squares are due to the laser plasma.

phase and is thought to arise from a dynamic effect. As the motion of the fluorine atoms about uranium in UF_7^- increases with temperature, the symmetry of the group increasingly averages out to pseudo-D_{5h}. This trend is shown up in the departure from this symmetry as the temperature decreases, which results in appearance of a shoulder on the band at 440 cm^{-1} and two weak bands at 500 and 550 cm^{-1}.

As the temperature decreases to ~20 °C, i.e., the sample reaches the low-symmetry crystalline phase, the Raman spectrum of KUF_7 displays a larger number of narrower bands (spectrum III). A further change of the spectrum is obtained (spectrum II) by aging or by a weak transitory thermal activation of the solid, for instance, through a short pulse of energy from the argon ion laser tuned to 200 mW followed by return to the previous power (~20 mW). It is then thought that spectrum III is in fact representative of a metastable state of KUF_7, which most likely comes from a previous cooling of the solid, the stable form being that one corresponding to spectrum II. It is noticed that the infrared spectrum is closely related to the Raman spectrum II probably as a result of the beam temperature effect. On the other hand, spectrum III is related to the spectrum recorded at −138 °C (spectrum IV). Again, as no phase change has been found in this temperature range, the difference between the two spectra is attributed to a change in the molecular motion rate. This slowing down of the motion at low temperature is reversed with an increase of temperature. Spectrum II would then be representative of a thermodynamically nonequilibrated metastable state in which superfreezing of the motion is taking place. Concerning the structural point of view, it is possible that with an increase in the molecular motion rate, the equilibrium interatomic distances are spread out over a wider variety of values. As a result, small inequivalencies of the fluorine atoms are lost, creating, in general, two different sets of atoms, one set containing two atoms and the other set containing five atoms, as required for the proposed pseudo-D_{5h} symmetry model. At

Table IV. X-Ray Data for the Potassium, Nitrosyl, Ammonium, Rubidium, and Cesium Octafluorouranates

K_2UF_8			$(NO)_2UF_8$			$(NH_4)_2UF_8$			Rb_2UF_8			Cs_2UF_8		
d, Å	Intensity	*hkl*	*d*, Å	Intensity	*hkl*	*d*, Å	Intensity	*hkl*	*d*, Å	Intensity	*hkl*	*d*, Å	Intensity	*hkl*
5.43	ms	110	5.46	m	110	7.46	w	011	7.52	w	011	5.90	mw	110
5.13	s	021	5.29	ms	021	6.23	w	100	6.36	vw	100	5.57	m	021
4.60	ms	111	4.64	m	111	5.60	s	110	5.64	m	110	4.96	mw	111
4.35	m	002	4.41	mw	002	5.32	s	021	5.36	s	021	4.69	mw	(030), 120
3.50	w diffuse	102	3.67	mw	022	5.13	vw	(101)	4.78	m	111	4.16	mw	031
3.47	m	130	3.57	m	130	4.80	s	111	4.51	mw	(030)	3.78	s	130
3.40	m	112	3.44	ms	112	4.60	vw	120	4.39	w	002	3.65	m	112
3.24	m diffuse	131, 040	3.31	m	040, 113	4.49	mw	002, (030)	4.10	w	121	3.50	m	131, 040
3.015	mw	200	3.007	w	200	3.64	m	130	4.03	w	031	3.305	mw	122
2.728	f	220, 132	2.782	w	211, 132	3.52	mw	112	3.63	vs	130	3.217	mw	200
2.653	vw	023	2.699	vw	023	3.36	ms	131, 040	3.51	m	112	2.937	vw	220, 132
2.604	mw diffuse	221	2.659	vw	(050), 042	3.15	w	200	3.36	ms	040, 131	2.802	vw	221, 050
2.575	mw	(050), 042	2.628	mw	221	2.928	w	013	3.167	vw	122	2.665	vw	230, 202
2.492	w	202	2.602	m	113	2.905	w	211	2.820	w	141, 132	2.558	w	231
2.433	vw	212	2.490	mw	230, 202	2.820	w	132, 141	2.688	mw	023	2.489	w	222, 151
2.371	w	231	2.440	mw	212, 150	2.712	mw	(103), 221	2.561	w	202	2.313	m	043, 004, 232
2.321	vw	222	2.352	w	151	2.649	w	113	2.460	mw	142, 033	2.260	mw	061
2.285	w	151	2.332	w	222	2.575	w	230	2.387	mw	151, 222	2.199	w	213
2.241	vw	133	2.277	w	052	2.509	w broad	123, 033	2.285	vw	133	2.137	ms	161
2.202	w	240, 052	2.236	w	240	2.459	mw	150	2.225	ms	232, 241	2.125	w broad	250, 242, 223
2.156	mw	043	2.216	w	004, 043	2.381	w	151	2.164	m	152, 014	1.987	w	153, 134
2.083	mw	061	2.161	mw	232, 241	2.293	mw	052, 240	2.052	m	114, 250	1.959	mw	302
2.060	vw	213, 024	2.136	w	152	2.215	w broad	014, 241	2.034	m	(301), 242	1.917	vw	331
2.000	m	300, 223	2.055	w	114	2.161	mw	152, 061				1.880	mw	243, 204
1.967	m	161, 242	2.011	mw	223, 300	2.113	vw	104, 143				1.868	mw	214, 063
			1.997	mw	250	2.065	mw	223				1.852	mw	144, 261
			1.940	w	251	2.045	mw	(301), 250, 242						
			1.883	w	162, 134, 153	2.012	vw	034						
			1.813	vw	252, 170									
			1.783	ms	331									
			1.757	m	144									
Orthorhombic			Orthorhombic			Orthorhombic			Orthorhombic			Orthorhombic		
a = 6.038 ± 0.014 Å			a = 6.012 ± 0.005 Å			a = 6.305 ± 0.013 Å			a = 6.265 ± 0.016 Å			a = 6.480 ± 0.010 Å		
b = 12.899 ± 0.028 Å			b = 13.311 ± 0.011 Å			b = 13.431 ± 0.023 Å			b = 13.479 ± 0.037 Å			b = 14.036 ± 0.022 Å		
c = 8.728 ± 0.022 Å			c = 8.861 ± 0.008 Å			c = 9.018 ± 0.016 Å			c = 8.776 ± 0.021 Å			c = 9.272 ± 0.012 Å		

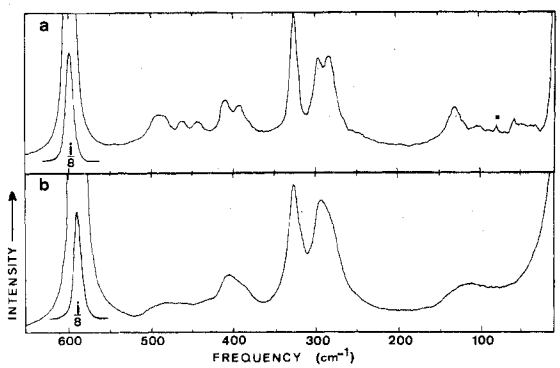

Figure 3. Raman spectra of solid K_2UF_8: (a) at room temperature (spectral slit width 3.2 cm^{-1}); (b) above room temperature (ca. +40 °C) (spectral slit width 3.2 cm^{-1}).

low temperature, the Raman spectrum of KUF_7 exhibits 21 bands, 18 of them being due to the internal vibrations. This number is in agreement with a symmetry at most equal to C_{2v}, since for this group 18 bands would be Raman active according to the selection rules.

In the octafluoro anion group, K_2UF_8 is also well representative of the marked effect of the temperature on the spectra. As seen in Figure 3, obtained at a temperature higher than room temperature (laser beam tuned to 500 mW), its Raman spectrum is very different from the spectrum obtained at, or very close to, room temperature (laser beam tuned to 5 mW). With a temperature increase, the shoulders in the bands at 295 and 408 cm^{-1} and the small bands around 470 cm^{-1} tend to disappear, whereas the highest frequency decreases from 598 to 591 cm^{-1}. The spectrum obtained at higher temperature is close to those obtained[27] for $(NO)_2UF_8$ and Cs_2UF_8 scanned near room temperature. It is noticed that the band seen around 325 cm^{-1} in these solids has not been observed for UF_8^{2-} in solution; therefore, as no other major change between the spectra of the solids and those in solution has been noticed, this band is assigned to a lattice vibration. In the same way, the bands found at ca. 100 and 40 cm^{-1} (the locations of which were found to be cation dependent) are also assigned to lattice vibrations. Therefore, at high temperature only four internal vibrations remain apparent in the Raman spectrum of K_2UF_8. Among the possible point group symmetries which have been reported in the literature for the XY_8 system, it is established from group theory that 4, 6, 7, 7, 15, and 21 bands should be Raman active and 2, 7, 5, 5, 9, and 17 infrared active for the groups O_h, D_{3d}, D_{4h}, D_{4d}, D_{2d}, and C_{2v}, respectively. Coincidences should occur only in the last two groups among the 9 and 17 bands given for D_{2d} and C_{2v}, respectively.

Therefore, as in the case for the heptafluorouranates which involved a motion effect, the Raman spectra of the octafluorouranates at high temperature look like they are due to species of a higher symmetry; that is, with only four Raman active internal vibrations, they correspond to a cubic arrangement (O_h group). At lower temperatures, the molecular motions are slowed down and the Raman and infrared spectra contain 10 and 7 bands, respectively, for the internal vibrations which, with four coincidences, are consistent with a symmetry at most equal to D_{2d} (dodecahedral arrangement).

Conclusions

Apart from having given additional data on the hepta- and octafluorouranates(VI), this study has shown the marked effect of the temperature, the media, and the cation size on the apparent structure of the anions studied.

It turns out that the actual geometry of these anions is easily disturbed by the external forces that are taking place in the various media either by solvation or crystalline field forces. The ease of distortion of these anions is most likely related to different conformations which are close to one another in energies. This effect can be paralleled to the fluorine internal exchange previously observed in the solids by NMR spectroscopy. From these findings in the solid state, UF_7^- and UF_8^{2-} have symmetries equal to or lower than C_{2v} and D_{2d}, respectively, and an increase in the temperature results in an increase of the internal molecular rearrangement rate. As a consequence, each fluorine atom is occupying a less definite vibrational level which results in an apparent equivalence of some atoms giving what has been called the pseudo-D_{5h} and O_h symmetries.

Because of the cation's interaction, the anion becomes distorted and a significant portion of the anion's formal negative charge is localized on one of the fluorine atoms. It is worth noting that such a mechanism could account for the F^- diffusion motion observed for $NOUF_7$ by NMR studies.[28] Such a diffusion motion, which has not been found for the alkali metal salts, has been assumed[28] to be due to the transient molecule NOF with the F^- ion being allowed to pass from one UF_7^- group to another in this manner. It should be noticed that according to our experimental data, the anion electronic cloud polarization results in a less symmetric structure for the anion associated to the smaller cations. On the other hand, the trend in the anion–cation interaction is also shown in the data concerning the relative thermal stabilities. Taking for instance the complex $NaUF_7$, for which the cation–anion interaction is expected to be the strongest, the distortion of the UF_7^- ion results in a significant ionic character for one of the fluorine atoms and consequently a relatively covalent bond for the other U–F bonds. From this, UF_6 is able to escape at relatively low temperature leaving Na_2UF_8, whereas an anion–cation interaction likely also occurs in this compound in such a way that UF_6 is given off on heating, leaving only the alkali metal fluoride. Conversely for $CsUF_7$, the first step occurs at higher temperature than for $NaUF_7$, leaving also the octafluorouranate. But this time the alkali metal fluoride interaction taking place in this salt is too weak to balance the mean U–F bond strength and consequently the anion keeps its entity up to a temperature at which the U–F bond is broken (due to its relative weakness), fluorine is given off, and Cs_2UF_7 is left as a solid residue.

To summarize, this study has shown an anion–cation interaction assumption to be able to explain the main trends observed in the experimental data of the properties studied.

Acknowledgment. We are pleased to acknowledge the help of Dr. J. C. Barral for his contribution to the Raman spectra, Mr. J. L. Person for his contribution to the chemical synthesis, Mrs. C. Makram, G. Derost, and T. Coquin for the chemical analysis, Mrs. M. Lance for her contribution to the x-ray work, and Drs. P. Rigny and P. Plurien for their stimulating discussions.

Registry No. $NOUF_7$, 59915-66-1; $CsUF_7$, 26297-22-3; KUF_7, 19610-56-1; $NaUF_7$, 19610-57-2; NH_4UF_7, 59982-81-9; $RbUF_7$, 59982-82-0; Na_2UF_8, 17499-61-5; K_2UF_8, 17499-60-4; $(NO)_2UF_8$, 59982-84-2; $(NH_4)_2UF_8$, 59992-13-1; Rb_2UF_8, 59982-85-3; Cs_2UF_8, 17476-96-9.

References and Notes

(1) On leave from Argonne National Laboratory.
(2) O. Ruff and F. Eisner, *Ber.*, **38**, 742 (1905).
(3) O. Ruff and F. Eisner, *Ber.*, **40**, 2926 (1907).
(4) O. Ruff and A. Heinzelmann, *Z. Anorg. Allg. Chem.*, **72**, 63 (1914).
(5) H. Martin, A. Albers, and H. P. Dust, *Naturwissenschaften*, **33**, 370 (1946).
(6) Hurd, U.S. Atomic Energy Commission Report AECD 4328 (1950).
(7) H. Martin, A. Albers, and H. P. Dust, *Z. Anorg. Allg. Chem.*, **265**, 128 (1951).
(8) Worthington, Industrial Group (United Kingdom Atomic Energy Authority) Report R/CA, 200 (1957).
(9) N. S. Nikolaev and V. F. Sukhoverkhov, *Dokl. Akad. Nauk SSSR*, **136**, 621 (1961).

(10) B. Volasek, *Croat. Chem. Acta*, **33**, 181 (1961).
(11) J. R. Geichman, P. R. Ogle, and L. R. Swaney, Goodyear Atomic Corporation Report GAT-T-809 (1961).
(12) I. Sheft, H. H. Hyman, R. Adams, and J. J. Katz, *J. Am. Chem. Soc.*, **83**, 291 (1961).
(13) U.S. Patent 3 039 846 (1962).
(14) J. R. Geichman, E. A. Smith, and P. R. Ogle, *Inorg. Chem.*, **2**, 1012 (1963).
(15) S. Katz, Oak Ridge National Laboratory Report ORNL 3497 (1964).
(16) S. Katz, *Inorg. Chem.*, **3**, 1958 (1964).
(17) L. McNeese, Oak Ridge National Laboratory Report ORNL 3494 (1964).
(18) J. G. Malm, H. Selig, and S. Siegel, *Inorg. Chem.*, **5**, 130 (1966).
(19) S. Katz, *Inorg. Chem.*, **5**, 666 (1966).
(20) I. Peka, *Collect. Czech. Chem. Commun.*, **37**, 4245 (1966).
(21) I. Peka, *Collect. Czech. Chem. Commun.*, **31**, 4469 (1966).
(22) I. Peka, *Collect. Czech. Chem. Commun.*, **32**, 426 (1967).
(23) A. T. Sadikova and N. S. Nikolaev, *Atomnaia Energuia*, **25**, 422 (1968).
(24) A. T. Sadikova, G. G. Sadikov, and N. S. Nikolaev, *Atomnaia Energuia*, **26 (3)**, 239 (1969).
(25) G. Besnard, A. J. Dianoux, O. Hartmanshenn, H. Marquet-Ellis, and N. H. Nghi, *Commis. Energ. At.* [*Fr.*], *Rapp.*, R-3732 (1969).
(26) A. Paillet, Thesis, Lyon, France, 1972.
(27) R. Bougon, R. M. Costes, J. P. Desmoulin, J. Michel, and J. L. Person, *Inorg. Nucl. Chem. Suppl.*, 99 (1976).
(28) P. Charpin, J. Michel, and P. Rigny, *Inorg. Nucl. Chem. Suppl.*, 131 (1976).
(29) These molar ratios are relative to the initial amount of materials, and due to a possible precipitation of a solid complex, e.g., MUF_7 or M_2UF_8; the actual composition may deviate from these figures.
(30) R. Bougon, unpublished data. Since this work, we have been aware of the work of J. Berry et al. on the oxidizing and fluoride ion acceptor properties of UF_6 in acetonitrile which is in agreement with our findings.
(31) A. Prescott, D. W. A. Sharp, and J. M. Winfield, *J. Chem. Soc.*, Dalton *Trans.*, 934 (1975).
(32) A. Prescott, D. W. A. Sharp, and J. M. Winfield, *J. Chem. Soc., Dalton Trans.*, 936 (1975).
(33) E. L. Muetterties, *Inorg. Chem.*, **4**, 769 (1965).
(34) A. J. Dianoux and P. Rigny, *J. Phys.*, **29**, 791 (1968).
(35) A. J. Dianoux, Thesis, Lyon, 1969.
(36) J. L. Person, Thesis CNAM, Paris, 1975.
(37) R. A. Penneman, G. D. Sturgeon, L. B. Asprey, and F. H. Kruze, *J. Am. Chem. Soc.*, **87**, 5803 (1965).
(38) J. L. Hoard, *J. Am. Chem. Soc.*, **61**, 1252 (1939).
(39) G. L. Brown and L. A. Walker, *Acta Crystallogr.*, **20**, 220 (1966).
(40) Pr. N. Bartlett, private communication.
(41) S. P. Beaton, Ph.D. Thesis, University of British Columbia, 1966.
(42) E. G. Ippolitov and P. A. Koz'min, *Dokl. Akad. Nauk SSSR*, **5**, 1081 (1962).

Contribution from Bell Laboratories,
Murray Hill, New Jersey 07974

Photoacoustic Spectroscopy of Iridium Carbonyl Halide Linear-Chain Conductors

A. ROSENCWAIG, A. P. GINSBERG,* and J. W. KOEPKE

Received April 12, 1976 AIC60281T

Optical studies of polycrystalline linear-chain conductors are of considerable current interest. However, these materials are generally highly light-scattering and thus difficult to study by conventional optical transmission or reflection techniques. Photoacoustic spectroscopy offers a highly effective means for obtaining optical spectra on such materials, and we report here the first photoacoustic study of this class of materials in the 250–1000-nm range, in particular, of the compounds $K_{0.60}Ir(CO)_2Cl_2 \cdot 0.5H_2O$, $K_{0.98}Ir(CO)_2Cl_{2.42} \cdot 0.2CH_3COCH_3$, $(TTF)_{0.61}Ir(CO)_2Cl_2$ (TTF = tetrathiafulvalenium), and $Cs_{0.60}Ir(CO)_2Br_2$. These compounds contain conducting linear chains of square-planar *cis*-$[Ir(CO)_2X_2]^{0.6-}$ (X = Cl, Br) units. Their photoacoustic spectra show three absorption bands below 650 nm at 2.3, 2.9, and ~3.4 eV, which are assigned as metal-to-ligand charge-transfer transitions from the a(yz) and b(xz) metal orbitals to the predominantly ligand CO b(π^*, $6p_z$) orbital. Above 650 nm the spectrum rises strongly toward the infrared region. This rise is the high-energy end of a broad absorption band extending from ~0.1 to 2 eV as subsequently shown by conventional infrared transmission spectroscopy. It is assigned as the transition from the $5d_{z^2}$ band to b(π^*, $6p_z$). The width and energy of this transition appear to depend upon chain length, exhibiting a significant broadening and shift to higher energy upon crushing of the sample. All of the observed linear-chain transitions are considerably red-shifted with respect to the corresponding transitions in nonchain $[Ir(CO)_2Cl_2]^-$. The red shift is attributed to interactions along the chain which raise the energy of a(yz), b(xz), and a(z^2) and lower the energy of b(π^*, $6p_z$).

Polycrystalline linear-chain conductors are generally highly light-scattering materials that are quite difficult to study in the optical region by conventional transmission or reflection spectroscopy. Since optical spectra of these materials are of considerable interest in providing information about their electronic structure, linear-chain conductors are excellent candidates for examination by the newly developed technique of photoacoustic spectroscopy.[1-3] In this paper we describe a photoacoustic study of the recently characterized compounds[4] $K_{0.60}Ir(CO)_2Cl_2 \cdot 0.5H_2O$, $K_{0.98}Ir(CO)_2Cl_{2.42} \cdot 0.2CH_3COCH_3$, $(TTF)_{0.61}Ir(CO)_2Cl_2$ (TTF = tetrathiafulvalenium), and $Cs_{0.60}Ir(CO)_2Br_2$. These compounds all contain conducting linear chains of square-planar *cis*-$[Ir(CO)_2X_2]^{0.6-}$ (X = Cl, Br) units, as illustrated in Figure 1.

In photoacoustic spectroscopy of solids, light absorbed by a solid sample is detected as an acoustic signal. It has been possible with this technique to obtain optical absorption spectra of almost any type of material, irrespective of whether the sample is crystalline or amorphous, a powder or a gel. Since only the *absorbed* light is converted to sound, scattered light, which presents such a severe problem when dealing with many solid materials by conventional means, presents no major problem in photoacoustic spectroscopy. Our results for the *cis*-$[Ir(CO)_2X_2]^{0.6-}$ linear chains show several notable features. In particular, we find that the linear chains have a near-ir absorption of variable frequency, apparently dependent on the chain length and not present in *cis*-$[Ir(CO)_2Cl_2]^-$ in the absence of chain formation. Also, the uv–visible region absorption of the chain complex is significantly red-shifted in comparison to nonchain $[Ir(CO)_2Cl_2]^-$, contrary to what might be expected in view of the higher Ir oxidation state in the chain complex. These effects are attributed to metal–metal interaction along the chain axis which results in band formation and raises the energy of the d levels from which the observed transitions originate.

Experimental Section

$K_{0.60}Ir(CO)_2Cl_2 \cdot 0.5H_2O$, $K_{0.98}Ir(CO)_2Cl_{2.42} \cdot 0.2CH_3COCH_3$, $(TTF)_{0.61}Ir(CO)_2Cl_2$, and $Cs_{0.60}Ir(CO)_2Br_2$ were prepared and characterized as described previously.[4] $(C_6H_5)_4As[Ir(CO)_2Cl_2]$ was prepared by the method of Forster[5] and characterized by its ir spectrum. Photoacoustic spectra in the range 250–1000 nm were obtained as described elsewhere;[1-3] the polycrystalline powders were studied both before and after grinding in an agate mortar. The absorption spectrum of $K_{0.98}Ir(CO)_2Cl_{2.42}$ in the region 600–17 000 nm was also determined with a Cary Model 14 R spectrophotometer (600–2500 nm) and a Perkin-Elmer Model 457 IR spectrophotometer